

Surface Molecular Imprinting on Silica-Coated CdTe Quantum Dots for Selective and Sensitive Fluorescence Detection of p-aminophenol in Water

Xialin Lu¹ · Fangdi Wei¹ · Guanhong Xu¹ · Yanzi Wu¹ · Jing Yang¹ · Qin Hu¹ 

Received: 25 June 2016 / Accepted: 3 October 2016 / Published online: 13 October 2016
© Springer Science+Business Media New York 2016

Abstract In this paper, a selective and sensitive sensor for the determination of p-aminophenol (PAP) was developed by grafting molecularly imprinted polymers (MIPs) on the surface of silica-coated CdTe quantum dots (CdTe@SiO₂@MIPs). The obtained CdTe@SiO₂@MIPs were characterized by X-ray powder diffraction, Fourier transform infrared spectroscopy, transmission electron microscopy and fluorescence spectroscopy. The fluorescence intensity of CdTe@SiO₂@MIPs was more strongly quenched by PAP than that of the structural analogues of PAP. Under the optimal conditions, the fluorescence intensity of the CdTe@SiO₂@MIPs decreased sensitively with the increase of PAP concentration in the range of 0.05–50 μM. The limit of detection was 0.02 μM ($3\sigma/K_{sv}$). The sensor was successfully used to determine PAP in tap and lake water samples, and the average recoveries of PAP at various spiking levels ranged from 97.33 % to 103.3 % with relative standard deviations below 20 %.

Keywords Silica-coated CdTe quantum dots · Surface molecular imprinting · p-aminophenol · Fluorimetry

Introduction

Luminescent semiconductor quantum dots (QDs) have attracted worldwide increasing attention and been widely used

as fluorescent probes in recent decades due to their excellent optical properties, such as broad excitation spectra, narrow and tunable emission spectra, quantum size effect, good photostability, high luminescence efficiency and so on [1–3]. However, lack of selectivity of QDs based probes was commonly reported, and the study on the development of novel and selective QDs based sensors is a current focus.

Molecularly imprinted polymers (MIPs) are tailor-made synthetic receptors, prepared by the copolymerization of functional monomers and crosslink agents in the presence of template molecules. After removal of the template, definite cavities, specific to both shape and chemical functionality of the template, are left, and thus MIPs show excellent affinity to the template molecules over their structural analogs [4–6].

Anchoring MIPs layer on the surface of QDs (QDs@MIPs) is a promising way to obtain QDs based probes with high selectivity and sensitivity. MIPs would recognize the analyte, and the fluorescence intensity of QDs would change according to the concentration of the bound analyte. The concentration of analyte can then be converted into optical signals and detected directly by fluorimetry [7–22]. Li et al. [23] reported molecularly imprinted silica nanospheres embedded CdSe QDs for highly selective and sensitive optosensing of pyrethroids. Fang et al. [24] prepared a novel MIPs on CdSe/ZnS QDs for highly selective detecting of mycotoxin zearalenone in cereal samples. Chantada-Vázquez et al. [25] synthesized MIPs coated Mn-doped ZnS QDs for specific fluorescent recognition of cocaine.

p-aminophenol (PAP) is an important materials in various fields, such as medicine, dyes, plastics, feeding stuff, antioxidants and artificial tanning agents. As a result, large amounts of PAP are inevitably released into the environment as a pollutant [26]. PAP is toxic and irritable to the eyes, skin and respiratory system, and the target sites of PAP in the body are blood and the kidneys. PAP is also very toxic to aquatic organisms and may cause long-term adverse effects in the

Xianlin Lu and Fangdi Wei contributed equally to this work.

✉ Qin Hu
huqin@njmu.edu.cn

¹ School of Pharmacy, Nanjing Medical University, Nanjing 211166, China

aquatic environment [27, 28]. The determination of PAP is an important content of environmental monitoring. HPLC is the most common method for the detecting of PAP [29–31], but the method requires expensive instrumentation, and highly trained technical staff to perform the analysis. Therefore, it is very necessary to develop a simple and reliable analytical method for the determination of PAP. In recent years, various techniques have been developed to determine PAP, such as electrochemical method [32–37], surface enhanced Raman scattering [38] and fluorimetry [39]. However, no literature has reported the application of QDs@MIPs to determine PAP.

In this paper, MIPs layer was grafted on the surface of CdTe@SiO₂ QDs (CdTe@SiO₂@MIPs) to develop a selective and sensitive sensor for rapid determination of PAP in water. CdTe@SiO₂ QDs were prepared by the one-pot method, and CdTe@SiO₂@MIPs were synthesized by the surface modification method. The CdTe@SiO₂@MIPs were characterized by X-ray powder diffraction, Fourier transform infrared spectroscopy (FT-IR), transmission electron microscopy (TEM) and fluorescence spectroscopy. The CdTe@SiO₂@MIPs sensor was finally applied to the determination of PAP in tap and lake water samples.

Materials and Methods

Reagents

Tellurium powder (Te), sodium borohydride (NaHB₄), cadmium acetate, tetraethylorthosilicate (TEOS) and ethanol were provided by Sinopharm chemical reagent Co. Ltd. (Shanghai, China). PAP, 1,4-diaminobenzene, p-benzenediol, 1,3-benzenediol, Mercaptopropionic acid (MPA), 3-aminopropyltriethoxysilane (APTES) were purchased from Sigma-Aldrich chemical company (St. Louis, MO, USA). Ultrapure water was obtained from a PURELAB Classic water purification machine (PALL, USA). All reagents used above were of at least analytical grade.

Apparatus

Fourier transform infrared (FT-IR) spectra were recorded using a Tensor-27 FT-IR spectrometer (Bruker, Germany) with a resolution of 2 cm⁻¹ and a spectral range of 4000–400 cm⁻¹. Fluorescence spectra were recorded on an F-4600 spectrophotometer (Hitachi, Japan) and the measurements were performed with the excitation wavelength at 370 nm. UV-vis absorption spectra were obtained using a UV-2450 UV-vis spectrophotometer (Shimadzu, Japan). X-ray diffraction (XRD) spectra were collected on a D1 SYSTEM X-ray diffractometer (Bebe, Britain). Transmission electron microscopy (TEM) images were recorded on a JEM-200CX microscope (JEOL, Japan). All the spectral measurements were carried out at room temperature.

Synthesis of CdTe@SiO₂ QDs

CdTe@SiO₂ QDs were prepared by a one-pot method according to the reference [40]. Firstly, 19.10 mg of Te powder and 34.00 mg of NaHB₄ were added to a 50 mL three-necked flask. After purged with nitrogen for 30 min, 5.0 mL of ultra-pure water was added to the flask. The mixture was stirred under nitrogen at room temperature until NaHTe aqueous solution was obtained. Secondly, NaHTe solution was introduced into N₂-saturated Cd²⁺ aqueous solution (2.0 mM) at pH 9 ~ 10 in the presence of MPA (4.8 mmol) at 90 °C. Then, 3.5 mL of TEOS was injected into the mixture, and the mixture was refluxed for 5 h. Finally, the CdTe@SiO₂ QDs solution was concentrated to 1/4 of the original volume and precipitated with ethanol. The CdTe@SiO₂ QDs were centrifuged and washed with absolute ethanol repeatedly. After purification, the CdTe@SiO₂ QDs were dried at 60 °C for 24 h under a vacuum.

Synthesis of CdTe@SiO₂@MIPs

200 mg of the above prepared CdTe@SiO₂ QDs, 10 mL of ethanol and 33 mg of PAP were added into a 50 mL three-necked flask. The mixture was stirred under nitrogen at room temperature for 20 min. Then, 140 μL of APTES (functional monomers) was added to the mixture. After stirred for 30 min, 535 μL of TEOS (crosslink agents) was added and the mixture was kept stirring for 10 min. At last, 500 μL of 6.25 % NH₃·H₂O was added and stirred for 20 h. The as-prepared CdTe@SiO₂@MIPs were centrifuged, and sequentially washed with ethanol and ultra-pure water for several times until the template could not be monitored by UV-vis. The non-imprinted polymers (NIPs) were synthesized in the same way except for the addition of PAP.

Determination of Photoluminescent Quantum Yield

The photoluminescent quantum yield (PLQY) of CdTe@SiO₂ QDs was calculated as the following equation [41]:

$$\varphi_x = \varphi_s \cdot \frac{A_s}{A_x} \cdot \frac{F_x}{F_s} \cdot \left(\frac{n_x}{n_s} \right)^2$$

Where, the subscripts “x” and “s” denote sample and standard, respectively. *A* is the absorbance of the solution at the exciting wavelength (≤0.05). *F* is the integrated fluorescence intensity. *n* is the refractive index of the solvent. Rhodamine 6G was selected as the standard. The solvents for CdTe@SiO₂ QDs and rhodamine 6G were ultra-pure water and ethanol, respectively.

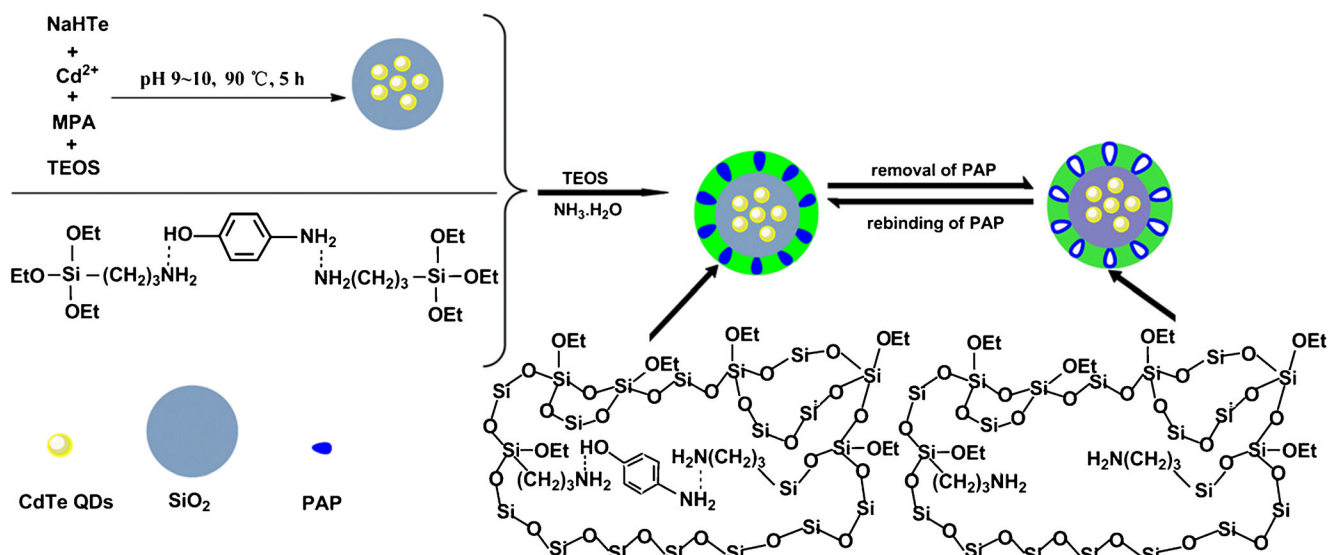


Fig. 1 Schematic illustration of fabricating CdTe@SiO₂@MIPs

Fluorescence Measurement

0.2 mL of CdTe@SiO₂@MIPs suspension, 1.0 mL of 0.1 M Tris-HCl buffer solution (pH 10.0), and 1.0 mL of PAP standard solution were sequentially added to a test tube. The mixture was ultrasonicated for 10 min. Then, fluorescence measurement was carried out with the excitation wavelength of 370 nm. The slit widths of excitation and emission were both 5 nm. The photomultiplier tube voltage was set at 750 V.

Analysis of Samples

The water samples were collected from our laboratory tap water and a local lake. The samples were filtered through 0.45 μm filter membrane before detecting. The analysis of PAP was carried out by using the method described above.

Results and Discussion

Synthesis and Characterization of CdTe@SiO₂@MIPs

Synthesis of CdTe@SiO₂@MIPs

Figure 1 gave the schematic diagram for preparing CdTe@SiO₂@MIPs. The preparation process included formation of CdTe@SiO₂ QDs, assembly of APTES and PAP, polymerization of recognizing cavities on the surface of CdTe@SiO₂ QDs, and elution of template molecules.

Coating QDs with silica can not only protect QDs from the environment, but also provide silicon hydroxyl groups which are needed in sequentially introducing the functional monomer and imprinting process. In our experiment, CdTe@SiO₂ QDs were prepared using a one-pot method by adding TEOS directly into the mixture of NaHTe, Cd²⁺, MPA and NaOH at

Fig. 2 TEM images of CdTe@SiO₂ QDs (a) and CdTe@SiO₂@MIPs (b)

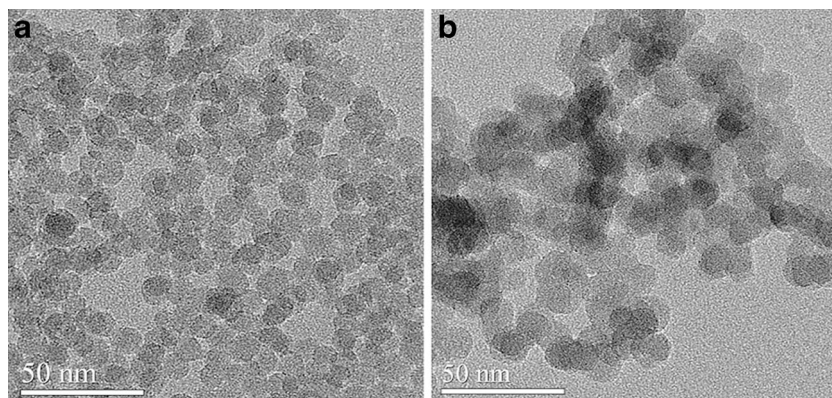
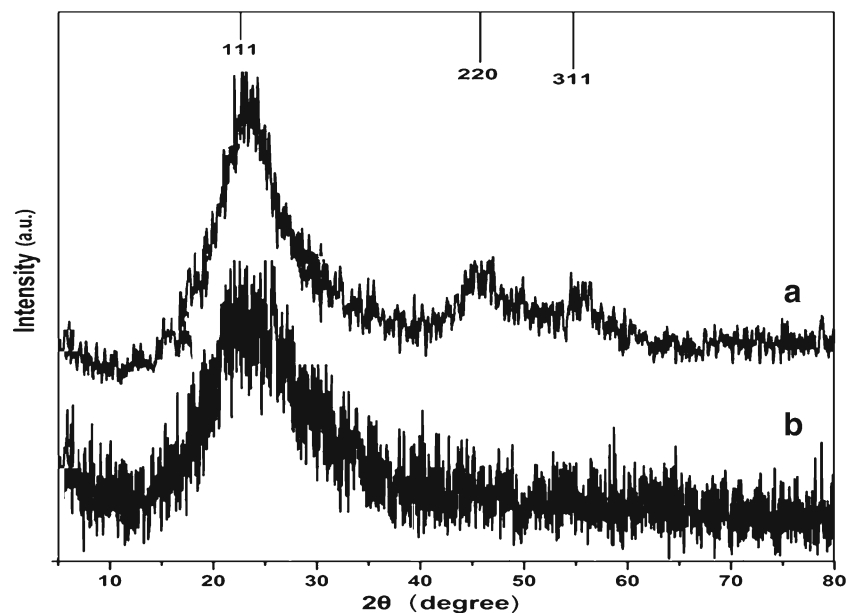


Fig. 3 XRD patterns of CdTe@SiO₂ QDs (a) and CdTe@SiO₂@MIPs (b)



90 °C. MIPs layer was grafted on the surface of the obtained CdTe@SiO₂ QDs via a surface molecularly imprinting process. APTES was used as a functional monomer, and incubated with PAP to form pre-polymers via strong non-covalent interaction. The resultant pre-polymers were further immobilized onto the surface of CdTe@SiO₂ QDs by the silanization reaction. Through the hydrolysis and condensation reaction of APTES and TEOS, the molecularly imprinting polymers were finally formed, in which the cavities for recognizing PAP were assembled via -Si-O- linkage by using NH₃·H₂O as a catalyst. Prior to the removal of PAP, the fluorescence intensity of CdTe@SiO₂@MIPs was 45.9 % of that of CdTe@SiO₂@NIPs. After several cycles of washing, the fluorescence intensity of CdTe@SiO₂@MIPs was increased to 94.5 % of that of CdTe@SiO₂@NIPs.

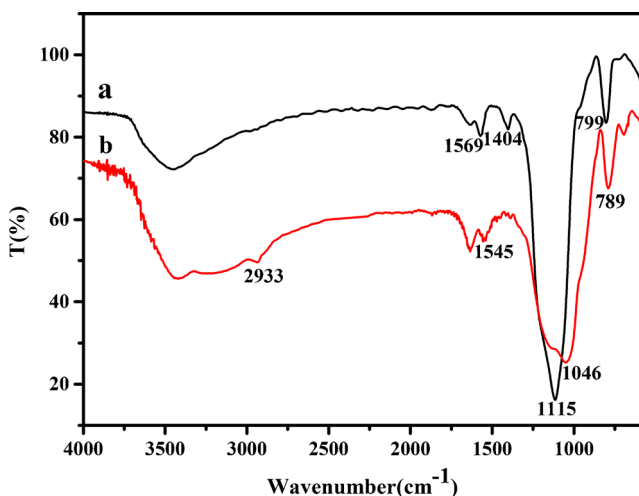


Fig. 4 FT-IR spectra of CdTe@SiO₂ QDs (a) and CdTe@SiO₂@MIPs (b)

Characterization of CdTe@SiO₂@MIPs

The morphology of CdTe@SiO₂ QDs and CdTe@SiO₂@MIPs was determined by TEM. As shown in Fig. 2, CdTe@SiO₂ QDs and CdTe@SiO₂@MIPs were nearly uniform in size, well-dispersed and spherical. The diameters of CdTe@SiO₂ QDs and CdTe@SiO₂@MIPs were about 10 and 15 nm, respectively.

XRD was used to observe the crystalline structures of CdTe@SiO₂ QDs and CdTe@SiO₂@MIPs (Fig. 3). The diffraction patterns of the two materials were consistent with that of bulk cubic CdTe structure [42], while the peak intensity of (220) and (311) of CdTe@SiO₂@MIPs became weak due to the growth of the polymeric layer on the surface of CdTe@SiO₂ QDs.

To further confirm the successful anchoring of MIPs layer on the surface of CdTe@SiO₂ QDs, the FT-IR spectra of CdTe@SiO₂ QDs and CdTe@SiO₂@MIPs were studied. In

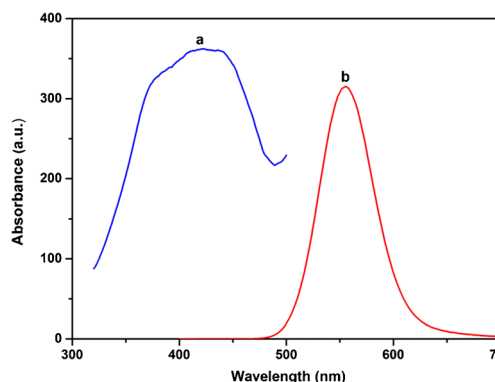


Fig. 5 Fluorescence excitation (a) and emission (b) spectra of CdTe@SiO₂ QDs

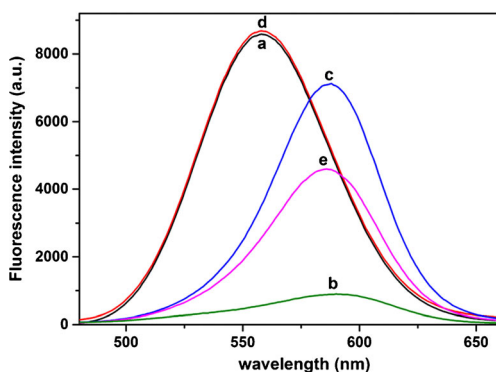


Fig. 6 Fluorescence spectra of CdTe@SiO₂ QDs (a), CdTe@SiO₂@MIPs before the removal of PAP (b), CdTe@SiO₂@MIPs after the removal of PAP (c), CdTe@SiO₂ QDs with addition of PAP (d) and CdTe@SiO₂@MIPs with addition of PAP (e)

Fig. 4a, the peaks located at 1569 and 1404 cm⁻¹ were the asymmetric and symmetric stretching bands of carboxylate anion of MPA, respectively, which was used as stabilizer in the preparation of CdTe@SiO₂ QDs; the peaks around 1115 and 799 cm⁻¹ showed the Si-O stretching and bending vibration of CdTe@SiO₂ QDs [43], respectively. After the imprinting process, aliphatic C-H stretching band (2933 cm⁻¹) appeared in Fig. 4b. Although C-H bonds existed in CdTe@SiO₂ QDs, the C-H stretching band did not appear in Fig. 4a due to the low sensitivity of IR spectrophotometry and relatively less number of C-H bonds in CdTe@SiO₂ QDs than that of CdTe@SiO₂@MIPs. The peaks of 1569 and 1404 cm⁻¹ of carboxylate anion of MPA which existed in the spectrum of CdTe@SiO₂ QDs disappeared in the spectrum of CdTe@SiO₂@MIPs, this suggested that MIPs layer was successfully grafted on the surface of CdTe@SiO₂ QDs and CdTe@SiO₂ QDs were tightly wrapped by MIPs layer. The

N-H band around 1545 cm⁻¹ in Fig. 4b resulting from APTES which was used as functional monomer in the synthesis of CdTe@SiO₂@MIPs, also proved the presence of MIPs on the surface of CdTe@SiO₂ QDs. Furthermore, after the imprinting process, the peaks of the stretching and bending vibration of Si-O shifted from 1115 cm⁻¹ to 1046 cm⁻¹ and 799 cm⁻¹ to 789 cm⁻¹, respectively. All the above results affirmed the successful synthesis of CdTe@SiO₂@MIPs.

Fluorescence Sensing of PAP by CdTe@SiO₂@MIPs

Fluorescence Characteristics of CdTe@SiO₂ QDs

Polymeric layer formed on the surface of QDs is not luminous and the optical properties of QDs@MIPs depend on the original QDs. So, QDs with excellent luminescence properties should be synthesized first. The common route for coating silica shell on QDs needs multistep complicated manipulations in which the QDs have to be presynthesized and separated before the SiO₂-coating reaction [44]. In our experiment, CdTe@SiO₂ QDs were prepared using a one-pot method [40] by adding TEOS directly into the mixture of NaHTe, Cd²⁺, MPA and NaOH at 90 °C. This could avoid the decrease of the PLQY of QDs during the separation process. Figure 5 showed that the CdTe@SiO₂ QDs synthesized in our experiment had a narrow full width at half maximum of 47 nm and broad excitation spectrum in the range of 375 to 450 nm. The PLQY of CdTe@SiO₂ QDs was as high as 81 %. The results indicated that the as-prepared CdTe@SiO₂ QDs had high optical qualities of narrow emission spectra, broad excitation spectra, and high photoluminescent quantum yield.

Fig. 7 Absorption spectrum of PAP (a) and emission spectrum of CdTe@SiO₂ QDs (b)

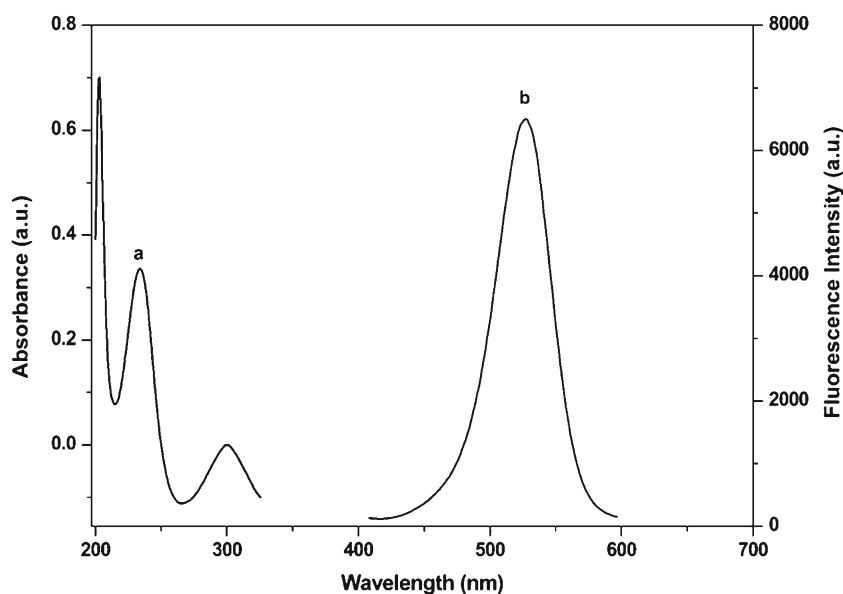


Table 1 Quenching constant of CdTe@SiO₂@MIPs and CdTe@SiO₂@NIPs for PAP and its structural analogues

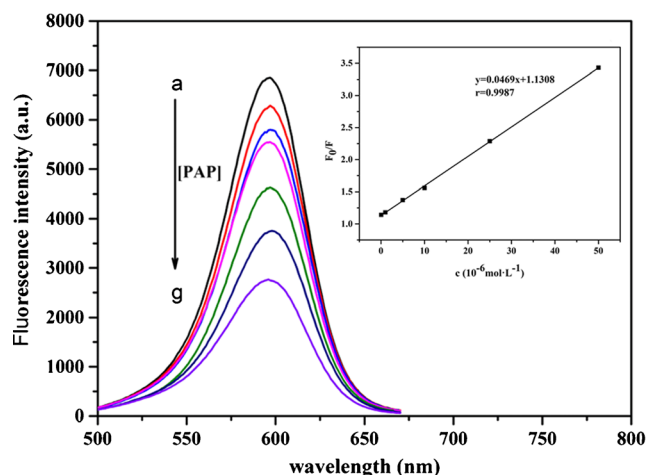
	$K_{sv, \text{MIPs}} (\text{M}^{-1})$	$K_{sv, \text{NIPs}} (\text{M}^{-1})$	IF
PAP	52,422	11,911	4.40
1,4-diaminobenzene	11,159	10,433	1.07
p-benzenediol	19,974	9933	2.01
1,3-benzenediol	15,687	11,011	1.42

Fluorescence Sensing of PAP by CdTe@SiO₂@MIPs

Figure 6 showed the changes in the fluorescence spectra of the original CdTe@SiO₂ QDs, CdTe@SiO₂@MIPs before and after the removal of PAP, CdTe@SiO₂ QDs with addition of PAP and CdTe@SiO₂@MIPs with addition of PAP. As shown in Fig. 6, the fluorescence intensity of the original CdTe@SiO₂ QDs (Fig. 6a) was almost quenched after the polymerization process and the fluorescence of the raw material of CdTe@SiO₂@MIP (Fig. 6b) was very weak. The fluorescence intensity of CdTe@SiO₂@MIPs was significantly increased (Fig. 6c) after the removal of the template, but didn't restore to the strength of the original CdTe@SiO₂ QDs. Compared with the original CdTe@SiO₂ QDs, the intensity of CdTe@SiO₂@MIPs decreased by 15 % due to the fact that the fluorescence of CdTe@SiO₂ QDs was slightly blocked by the MIPs layer. Moreover, the maximum emission wavelength of CdTe@SiO₂@MIPs also had an obvious red shift of 30 nm. It is well known that a single charge (Si-O groups, hydroxyl ions, or ammonium ions) close to the surface of QDs can generate an electric field that is sufficiently large to cause a red shift and significant quenching of the QDs emission. Thus, the fluorescence quenching and red shift of CdTe@SiO₂@MIPs were ascribed to the attachment of fully hydrolyzed and subsequently condensed APTES and TEOS to the surface of CdTe@SiO₂ QDs [45]. Meanwhile, the imprinting process led to the increase of the size of QDs, and red shift of the CdTe@SiO₂ QDs emission appeared due to the quantum size effect.

Table 2 Interfering effect of common metal ions

Substance	Ratio of substance to PAP	Change of fluorescence intensity (%)
NaCl	100	1.7
KCl	100	0.4
CaSO ₄	100	-1.9
FeCl ₃	100	1.0
ZnSO ₄	100	3.2
Al ₂ (SO ₄) ₃	50	0.8
CuSO ₄	50	-2.2

**Fig. 8** Fluorescence spectra of CdTe@SiO₂@MIPs at different concentrations of PAP

When PAP was present in CdTe@SiO₂ QDs, the fluorescence intensity of CdTe@SiO₂ QDs remained almost unchanged (Fig. 6d). However, the fluorescence intensity of CdTe@SiO₂@MIPs was quenched obviously when the same concentration of PAP was added (Fig. 6e). Because there was no spectral overlap between the absorption spectrum of PAP and the emission spectrum of CdTe@SiO₂ QDs (Fig. 7), energy transfer was therefore not a possible mechanism for the fluorescence quenching. The fluorescence quenching might involve charge transfer when PAP molecules interacted with the functional groups in the imprinting cavities by hydrogen bonding [46]. In addition, when PAP molecules entered into the cavities of CdTe@SiO₂@MIPs, they would block the light emitted by CdTe@SiO₂@MIPs just like shading plates.

Specificity and Interference Experiments

According to the references [47–51], the fluorescence quenching in this system followed the Stern-Volmer equation:

$$F_0/F = 1 + K_{sv}[Q]$$

Table 3 Determination of PAP in tap water and lake water (n = 3)

Samples	Added (μM)	Found (μM)	Recovery (%)	RSD (%)
Tap water	0	0	-	-
	0.150	0.154	102.7	18.0
	7.50	7.35	98.0	1.7
Lake water	0	0	-	-
	0.150	0.154	102.7	19.0
	7.50	7.30	97.3	3.7
	30.0	30.3	101.0	0.7

Where, F_0 and F are the fluorescence intensities in the absence and presence of quencher, respectively. $[Q]$ is the concentration of the quencher. K_{sv} is the quenching constant. K_{sv} and the imprinting factor (IF , the ratio of $K_{sv,MIPs}$ to $K_{sv,NIPs}$) are usually used to evaluate the sensitivity and selectivity of the sensor, respectively.

Table 1 exhibited that both K_{sv} and IF of CdTe@SiO₂@MIPs to PAP were about three times as much as that of CdTe@SiO₂@MIPs to the structural analogues of PAP. As special PAP recognition sites based on the size, shape, and location of the hydrogen bond of the binding cavity were grafted on the surface of CdTe@SiO₂@MIPs, PAP could easily reunite with CdTe@SiO₂@MIPs materials, causing obviously fluorescence quenching. For the other molecules, the imprinting sites were not match, so little fluorescence quenching was observed.

The K_{sv} of CdTe@SiO₂@NIPs to PAP and the analogues were similar, indicating that there were no selective binding cavities in CdTe@SiO₂@NIPs, and the molecules were retained on the NIPs shell through a non-specific process.

Meanwhile, in order to investigate the possibility of practical application of the CdTe@SiO₂@MIPs sensor in the determination of PAP in water, the interferences from common metal ions existing in water were tested under the optimal conditions. As shown in Table 2, they had basically no effect on the fluorescence intensity of CdTe@SiO₂@MIPs even at high concentrations.

All the above results indicated that the as-prepared CdTe@SiO₂@MIPs had high sensitivity and selectivity, and could be used as a fluorescent sensor for the determination of PAP in water.

Sensitivity of CdTe@SiO₂@MIPs Sensor

Under the optimal conditions, the fluorescence intensity of the CdTe@SiO₂@MIPs decreased sensitively with the increase of PAP concentration in the range of 0.05–50 μM (Fig. 8). The linear regression equation of CdTe@SiO₂@MIPs was $F_0/F = 1.1308 + 0.0469 [Q]$. The limit of detection (LOD) was defined as the concentration of PAP that quenched three times the standard deviation of the blank signal divided by the slope of the standard curve ($3\sigma/K_{sv}$), and the LOD was evaluated to be 0.02 μM.

Application to Water Sample Analysis

The sensing of PAP in water samples collected from our laboratory tap water and a local lake was carried out to investigate further the practical application of CdTe@SiO₂@MIPs sensor. Table 3 revealed that PAP was not detected in the collected water samples. The accuracy of the method was estimated by determining water samples spiked with three different

concentrations of PAP at 0.150, 7.50 and 30.0 μM. The recoveries were in the range of 97.33–103.3 % with the relative standard deviations less than 20 %, demonstrating the potential applicability of the CdTe@SiO₂@MIPs sensor for the quantification of PAP in real samples.

Conclusions

In summary, CdTe@SiO₂@MIPs fluorescence sensor was designed, synthesized and investigated for detection of PAP. The CdTe@SiO₂@MIPs showed uniform morphology, good dispersibility, fantastic binding capacity and selectivity for PAP. Selective and sensitive determination of PAP can be achieved on the basis of an electron-transfer-induced fluorescence quenching mechanism between CdTe@SiO₂@MIPs and PAP. The proposed method has a potential to be used to simply and fast monitor PAP in environmental water samples.

Acknowledgments This work was financially supported by the National Natural Science Foundation of China (No. 81171937).

References

- Sun QJ, Wang YA, Li LS, Wang DY, Zhu T, Xu J, Yang CH, Li YF (2007) Bright multicoloured light emitting diodes based on quantum dots. *Nat Photonics* 1(12):717–722
- Cui L, He XP, Chen GR (2015) Recent progress in quantum dot based sensors. *RSC Adv* 5(3–4):26644–26653
- Dehbozorgi A, Tashkhourian J, Zare S (2015) Fluorescence determination of warfarin using TGA-capped CdTe quantum dots in human plasma samples. *J Fluoresc* 25(6):1887–1895
- Liu HL, Fang GZ, Li CM, Pan MF, Liu CC, Fan C, Wang S (2012) Molecularly imprinted polymer on ionic liquid-modified CdSe/ZnS quantum dots for the highly selective and sensitive optosensing of tocopherol. *J Mater Chem* 22(37):19882–19887
- Zhao WH, Sheng N, Zhu R, Wei FD, Cai Z, Zhai MJ, Du SH, Hu Q (2010) Preparation of dummy template imprinted polymers at surface of silica microparticles for the selective extraction of trace bisphenol A from water samples. *J Hazard Mater* 179(1–3):223–229
- Xu SF, Lu HZ (2015) Ratiometric fluorescence and mesoporous structure dual signal amplification for sensitive and selective detection of TNT based on MIP@QD fluorescence sensors. *Chem Commun* 51(15):3200–3203
- Diltemiz SE, Say R, Büyüktiryaki S, Hür D, Denizli A, Ersöz A (2008) Quantum dot nanocrystals having guanosine imprinted nanoshell for DNA recognition. *Talanta* 75(4):890–896
- Wang HF, He Y, Ji TR, Yan XP (2009) Surface molecular imprinting on Mn-doped ZnS quantum dots for room-temperature phosphorescence optosensing of pentachlorophenol in water. *Anal Chem* 81(81):1615–1621
- Ge SG, Zhang CC, Yu F, Yan M, Yu JH (2011) Layer-by-layer self-assembly CdTe quantum dots and molecularly imprinted polymers modified chemiluminescence sensor for deltamethrin detection. *Sensor Actuat B-Chem* 156(1):222–227
- Zhang W, He XW, Chen Y, Li WY, Zhang YK (2011) Composite of CdTe quantum dots and molecularly imprinted polymer as a

- sensing material for cytochrome c. *Biosens Bioelectron* 26(5):2553–2558
11. Ye T, Lu SY, Hu QQ, Jiang X, Wei GF, Wang JJ, Lu JQ (2011) One-bath synthesis of hydrophilic molecularly imprinted quantum dots for selective recognition of chlorophenol. *Chin Chem Lett* 22(10):1253–1256
 12. Ge SG, Lu JJ, Ge L, Yan M, Yu JH (2011) Development of a novel deltamethrin sensor based on molecularly imprinted silica nanoparticles embedded CdTe quantum dots. *Spectrochim Acta A* 79(79):1704–1709
 13. Zhang W, He XW, Chen Y, Li WY, Zhang YK (2012) Molecularly imprinted polymer anchored on the surface of denatured bovine serum albumin modified CdTe quantum dots as fluorescent artificial receptor for recognition of target protein. *Biosens Bioelectron* 31(1):84–89
 14. Yang M, Han AJ, Duan JL, Li ZP, Lai YC, Zhan JH (2012) Magnetic nanoparticles and quantum dots co-loaded imprinted matrix for pentachlorophenol. *J Hazard Mater* 237–238(17):63–70
 15. Chen YP, Wang DN, Yin YM, Wang LY, Wang XF, Xie MX (2012) Quantum dots capped with dummy molecularly imprinted film as luminescent sensor for the determination of tetrabromobisphenol A in water and soils. *J Agric Food Chem* 60(42):10472–10479
 16. Kim YD, Jeon JB, Chang JY (2012) CdSe quantum dot-encapsulated molecularly imprinted mesoporous silica particles for fluorescent sensing of bisphenol A. *J Mater Chem* 22(45):24075–24080
 17. Liu HL, Fang GZ, Zhu HD, Li CM, Liu CC, Wang S (2013) A novel ionic liquid stabilized molecularly imprinted optosensing material based on quantum dots and graphene oxide for specific recognition of vitamin E. *Biosens Bioelectron* 47(10):127–132
 18. Li DY, He XW, Chen Y, Li WY, Zhang YK (2013) Novel hybrid structure silica/CdTe/molecularly imprinted polymer: synthesis, specific recognition, and quantitative fluorescence detection of bovine hemoglobin. *ACS Appl Mater Interfaces* 5(23):12609–12616
 19. Dan L, Wang HF (2013) Mn-doped ZnS quantum dot imbedded two-fragment imprinting silica for enhanced room temperature phosphorescence probing of domoic acid. *Anal Chem* 85(10):4844–4848
 20. Chao MR, Hu CW, Chen JL (2014) Comparative syntheses of tetracycline-imprinted polymeric silicate and acrylate on CdTe quantum dots as fluorescent sensors. *Biosens Bioelectron* 61(6):471–477
 21. Ren XH, Liu HC, Chen LG (2014) Fluorescent detection of chlorpyrifos using Mn(II)-doped ZnS quantum dots coated with a molecularly imprinted polymer. *Microchim Acta* 182(1):193–200
 22. Sadeghi S, Jahani M, Belador F (2016) The development of a new optical sensor based on the Mn doped ZnS quantum dots modified with the molecularly imprinted polymers for sensitive recognition of florfenicol. *Spectrochim Acta A* 159:83–89
 23. Li HB, Li YL, Cheng J (2010) Molecularly imprinted silica nanoparticles embedded CdSe quantum dots for highly selective and sensitive optosensing of pyrethroids. *Chem Mater* 22(8):2451–2457
 24. Fang GZ, Fan C, Liu HL, Pan MF, Zhu HD, Wang S (2014) A novel molecularly imprinted polymer on CdSe/ZnS quantum dots for highly selective optosensing of mycotoxin zearalenone in cereal samples. *RSC Adv* 4(6):2764–2771
 25. Chantada-Vázquez MP, Sánchez-González J, Peña-Vázquez E, Tabernero MJ, Bermejo AM, Bermejo-Barrera P, Moreda-Piñeiro A (2016) Synthesis and characterization of novel molecularly imprinted polymer-coated Mn-doped ZnS quantum dots for specific fluorescent recognition of cocaine. *Biosens Bioelectron* 75:213–221
 26. Beye H, Walter W (1997) *In organic Phys Chem*. Albion Publishing Ltd
 27. Bessems JGM, Vermeulen NPE (2001) Paracetamol (acetaminophen)-induced toxicity: molecular and biochemical mechanisms, analogues and protective approaches. *Crit Rev Toxicol* 31(1):55–138
 28. Harmon RC, Kinningham KK, Valentovic MA (2006) Pyruvate reduces 4-aminophenol in vitro toxicity. *Toxicol Appl Pharmacol* 213(2):179–186
 29. Schultz B (1984) Determination of 4-aminophenol in water by high-performance liquid chromatography with fluorescence detection. *J Chromatogr* 299(2):484–486
 30. Bloomfield MS (2002) A sensitive and rapid assay for 4-aminophenol in paracetamol drug and tablet formulation, by flow injection analysis with spectrophotometric detection. *Talanta* 58(6):1301–1310
 31. Wyszeccka-Kaszuba E, Warowna-Grzeskiewicz M, Fijalek Z (2003) Determination of 4-aminophenol impurities in multicomponent analgesic preparations by HPLC with amperometric detection. *J Pharm Biomed Anal* 32(5):1081–1086
 32. Yin HS, Ma Q, Zhou YL, Ai SY, Zhu LS (2010) Electrochemical behavior and voltammetric determination of 4-aminophenol based on graphene-chitosan composite film modified glassy carbon electrode. *Electrochim Acta* 55(23):7102–7108
 33. Fan Y, Liu JH, Yang CP, Yu M, Liu P (2011) Graphene-polyaniline composite film modified electrode for voltammetric determination of 4-aminophenol. *Sensor Actuat B-Chem* 157(2):669–674
 34. Neto JRM, Santos WJR, Lima PR, Tanaka SMCN, Tanaka AA, Kubota LT (2011) A hemin-based molecularly imprinted polymer (MIP) grafted onto a glassy carbon electrode as a selective sensor for 4-aminophenol amperometric. *Sensor Actuat B-Chem* 152(2):220–225
 35. Shiroma LY, Santhiago M, Gobbi AL, Kubota LT (2012) Separation and electrochemical detection of paracetamol and 4-aminophenol in a paper-based microfluidic device. *Anal Chim Acta* 725(9):44–50
 36. Lavanya N, Sudhan N, Kanchana P, Radhakrishnan S, Sekar C (2015) A new strategy for simultaneous determination of 4-aminophenol, uric acid and nitrite based on a graphene/hydroxyapatite composite modified glassy carbon electrode. *RSC Adv* 5(65):52703–52709
 37. Wang JS, Shi Z, Jin J, Liu Q, Zhang SH (2015) Determination of 4-aminophenol using a glassy carbon electrode modified with a three-dimensionally ordered macroporous film of polycysteine. *Microchim Acta* 182(3–4):823–829
 38. DeBleye C, Dumont E, Rozet E, Sacré PY, Chavez PF, Netchacovitch L, Piel G, Hubert P, Ziemons E (2013) Determination of 4-aminophenol in a pharmaceutical formulation using surface enhanced Raman scattering: from development to method validation. *Talanta* 116(22):899–905
 39. Dejaegher B, Bloomfield MS, Smeyers-Verbeke J, Vander Heyden Y (2008) Validation of a fluorimetric assay for 4-aminophenol in paracetamol formulations. *Talanta* 75(1):258–265
 40. Zhou L, Gao C, Hu XZ, Xu WJ (2010) One-pot large-scale synthesis of robust ultrafine silica-hybridized CdTe quantum dots. *ACS Appl Mater Interfaces* 2(4):1211–1219
 41. Grabolle M, Spieles M, Lesnyak V, Gaponik N, Eychmüller A, Resch-Genger U (2009) Determination of the fluorescence quantum yield of quantum dots: suitable procedures and achievable uncertainties. *Anal Chem* 81(15):6285–6294
 42. Hewa-Kasakarage NN, Gurusinge NP, Zamkov M (2009) Blue-shifted emission in CdTe/ZnSe heterostructured nanocrystals. *J Phys Chem C* 113(11):4362–4368
 43. Silverstein RM, Webster FX, Kiemle DJ (2005) *Spectrometric identification of organic compounds*. John Wiley & Sons, Inc
 44. Murase N, Yang P (2009) Anomalous photoluminescence in silica-coated semiconductor nanocrystals after heat treatment. *Small* 5(7):800–803

45. Wang LW (2001) Calculating the influence of external charges on the photoluminescence of a CdSe quantum dot. *J Phys Chem B* 105(12):2360–2364
46. Liu HL, Liu DR, Fang GZ, Liu FF, Liu CC, Yang YK, Wang S (2013) A novel dual-function molecularly imprinted polymer on CdTe/ZnS quantum dots for highly selective and sensitive determination of ractopamine. *Anal Chim Acta* 762(2):76–82
47. Zhang W, He XW, Li WY, Zhang YK (2012) Thermo-sensitive imprinted polymer coating CdTe quantum dots for target protein specific recognition. *Chem Commun* 48(2):1757–1759
48. Xu SF, Lu HZ, Li JH, Song XL, Wang AX, Chen LX, Han SB (2013) Dummy molecularly imprinted polymers-capped CdTe quantum dots for the fluorescent sensing of 2,4,6-trinitrotoluene. *ACS Appl Mater Interfaces* 5(16):8146–8154
49. Yang YQ, He XW, Wang YZ, Li WY, Zhang YK (2014) Epitope imprinted polymer coating CdTe quantum dots for specific recognition and direct fluorescent quantification of the target protein bovine serum albumin. *Biosens Bioelectron* 54(8):266–272
50. Ren XH, Chen LG (2015) Quantum dots coated with molecularly imprinted polymer as fluorescence probe for detection of cyphenothrin. *Biosens Bioelectron* 64:182–188
51. Wei FD, Wu YZ, Xu GH, Gao YK, Yang J, Liu LP, Zhou P, Hu Q (2014) Molecularly imprinted polymer based on CdTe@SiO₂ quantum dots as a fluorescent sensor for the recognition of norepinephrine. *Analyst* 139(22):5785–5792